

INTEGRATED DESIGN OF A MECHATRONIC SYSTEM

The Pressure Control in Common Rails

Paolo Lino and Bruno Maione

Dipartimento di Elettrotecnica ed Elettronica, Politecnico di Bari, via Re David 200, 70125, Bari, Italy

Keywords: Mechatronic systems, Virtual prototyping, AMESim[®], Modelling, Automotive control.

Abstract: This paper describes the integrated design of the pressure control in a common-rail injection system. Mechanical elements and the embedded controller are considered as a whole, using a multi-disciplinary approach to modelling and simulation. The virtual prototype, which provides the detailed geometrical/physical model of the mechanical parts, plays the role of a surrogate of a reference hardware prototype in reduced-order modelling, validation, and/or in tuning the control parameters. The results obtained by the proposed approach are compared and validated by experiments.

1 INTRODUCTION

The innovative characters of mechatronic systems lie with a special design process thinking about the mechanical parts and the embedded controllers as a whole. On the contrary, the traditional design of devices combining mechanical and electronic elements considers components belonging to different physical domain separately. Moreover controllers are conceived for already existing plants. Hence the physical properties and the dynamical behaviour of parts, in which energy conversion plays a central role, are not determined by the choices of the control engineers and therefore are of little concern to them. Their primary interests, indeed, are signal processing and information management, computer power requirements, choice of sensors and sensor locations, and so on. So it can happen that poorly designed mechanical parts do never lead to good performance, even in presence of advanced controllers. On the other hand, a poor knowledge of how controllers can directly influence and balance for defects or weaknesses in mechanical components does not help in achieving quality and good performance of the whole process. Aiming at an integrated design, in mechatronic systems the interactions among mechanical, electronic and information processing elements are considered in all the design steps, beginning with the early stages

(Stobart et al., 1999),(van Amerongen and Breedveld, 2003).

If the design choices must be made before assembling interacting parts of a physical prototype and if these parts belong to different physical domains (such as mechanics, electronics, hydraulics and control) the virtual prototyping approaches, which are surrogates for preliminary physical realizations, face many difficulties. The first one is due to the fact that each physical domain has specific modelling and simulation tools. Unfortunately, indeed, there is a gap between tools for evaluating the designed components in different domains. For example, mechanical engineers usually refer to finite element approaches/packages as an important tool for dimensioning mechanical parts and for evaluating their dynamical properties. Only after a complex order-reduction process (modal analysis) the so obtained models are reduced in a form suitable for the control analysis and design. On the other hand, control modelling tools are based on operators (transfer functions, frequency response) and/or on state equations descriptions, which, in many cases, do not have a straightforward connection with the critical parameters of physical design. However, it is clear that an appropriate modelling and simulation approach can not be fitted into the limitations of one formalism at time, particularly in the early stages of the design process. Hence, it is necessary a combination

of different methodologies in a multi-formalism approach to modelling supported by an appropriate simulation environment.

In mechatronic applications, the Bond Graphs introduced by (Paynter, 1960) provide a continuous system modelling approach, oriented to a class of interconnected and completely different systems and targeted to many user groups. Bond Graphs are very useful in analysing and designing components built from different energetic media and can represent dynamical systems at higher level of abstraction than differential equations (van Amerongen and Breedveld, 2003), (Ferretti et al., 2004).

In this paper, we referred to AMESim[®] (Advanced Modelling Environment for performing Simulations of engineering systems) (IMAGINE S.A., 2004) a Bond Graph-based, multi-domain modelling/optimization tool for the virtual prototyping of the physical/geometrical characteristics of a Compressed Natural Gas (CNG) injection system. In a first step, we used this tool to obtain a virtual prototype, as similar as possible to the actual final hardware. Then, with reference to this prototype, we also determined a reduced order model in form of transfer function and/or state space model, more suitable for analytical (or empirical) tuning of the pressure controller of the CNG injection systems. Using the virtual prototype in these early design stages enabled the evaluation of the influence of the geometrical/physical alternatives on the reduced model used for the controller tuning. Then, based on this reduced model, the controller settings were designed and adjusted in accordance with the early stages of the mechanical design process. Finally, the detailed physical/geometric model of the mechanical parts, created by the AMESim package, was exported and used as a module in a simulation program, which enabled the evaluation of the controller performance in the closed-loop system. In other words, the detailed simulation model surrogated for a real hardware.

2 THE INTEGRATED DESIGN APPROACH

In this paper, we consider the opportunity of integrating different models, at different level of details, and different design tools, to optimize the design of the mechanical and control systems as a whole. To sum up, the integrated design can take advantage of peculiarities of different specific software packages. The effectiveness of the approach is illustrated by means of a case study, the pressure control of a CNG injection system for internal combustion engines, which

represents a benchmark for the evaluation of performances of the approach. Experimental results give a feedback of benefits of the integration of the mechanical and control subsystems design.

The integrated design involves the development of a virtual prototype of the considered system using an advanced modelling tool (AMESim in this paper), which is employed for the analysis of the system performances during the different developing steps. Actually, the virtual prototype could be assumed as a reliable model of the real system. Further, a low order analytical model of the real system can be developed to simplify the controller design. Since AMESim can represent physical phenomena at different level of details, it is exploited to verify assumptions in building the analytical model. Then, the control system is designed using a specific software package, i.e. MATLAB/Simulink[®], and tested on the virtual prototype. The virtual prototype allows to perform safer, less expensive, and more reliable tests than using the real system.

3 APPLICATION EXAMPLE

We consider a system composed of the following elements (Fig. 1): a fuel tank, storing high pressure gas, a mechanical pressure reducer, a solenoid valve and the fuel metering system, consisting of a common rail and four electro-injectors. Two different configurations were compared for implementation, with different arrangements of the solenoid valve affecting system performances (i.e. cascade connection, figure 1(a), and parallel connection, Fig.1(b), respectively). Detailed AMESim models were developed for each of them, providing critical information for the final choice. Few details illustrate the injection operation for both layouts.

With reference to Fig. 1(a), the pressure reducer receives fuel from the tank at a pressure in the range between 200 and 20 bars and reduces it to a value of about 10 bar. Then the solenoid valve suitably regulates the gas flow towards the common rail to control pressure level and to damp oscillations due to injections. Finally, the electronically controlled injectors send the gas to the intake manifold for obtaining the proper fuel air mixture. The injection flow only depends on rail pressure and injection timings, which are precisely driven by the Electronic Control Unit (ECU). The variable inflow section of the pressure reducer is varied by the axial displacement of a spherical shutter coupled with a moving piston. Piston and shutter dynamics are affected by the applied forces: gas pressure in a main chamber acts on the

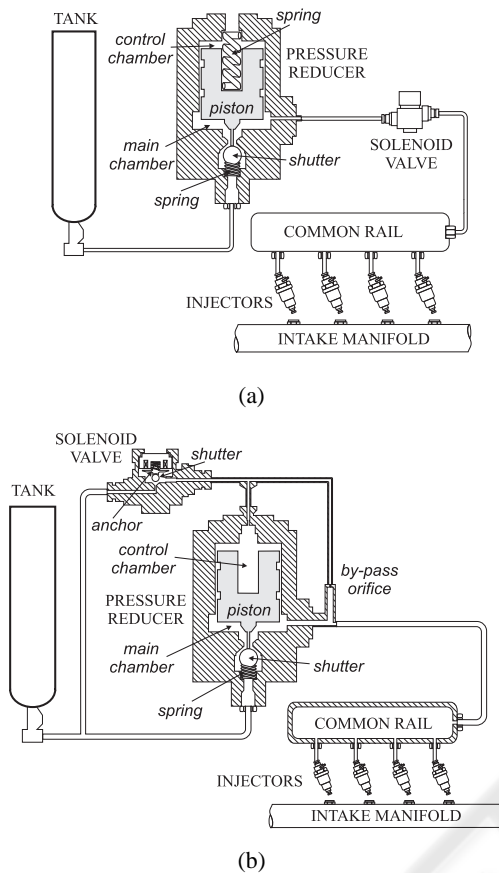


Figure 1: Block schemes of the common rail CNG injection systems; (a) cascade connection of solenoid valve; (b) parallel connection of solenoid valve.

piston lower surface pushing it at the top, and elastic force of a preloaded spring holden in a control chamber pushes it down and causes the shutter to open. The spring preload value sets the desired equilibrium reducer pressure: if the pressure exceeds the reference value the shutter closes and the gas inflow reduces, preventing a further pressure rise; on the contrary, if the pressure decreases, the piston moves down and the shutter opens, letting more fuel to enter and causing the pressure to go up in the reducer chamber (see (Maione et al., 2004) for details).

As for the second configuration (Fig. 1(b)), the fuel from the pressure reducer directly flows towards the rail, and the solenoid valve regulates the intake flow in a secondary circuit including the control chamber. The role of the force applied by the preloaded spring of control chamber is now played by the pressure force in the secondary circuit, which can be controlled by suitably driving the solenoid valve. When the solenoid valve is energized, the fuel en-

ters the control chamber, causing the pressure on the upper surface of the piston to build up. As a consequence, the piston is pushed down with the shutter, letting more fuel to enter in the main chamber, where the pressure increases. On the contrary, when the solenoid valve is non-energized, the pressure on the upper side of the piston decreases, making the piston to raise and the main chamber shutter to close under the action of a preloaded spring (see (Lino et al., 2006) for details).

On the basis of a deep analysis performed on AMESim virtual prototypes the second configuration was chosen as a final solution, because it has advantages in terms of performances and efficiency. To sum up, it guarantees faster transients as the fuel can reach the common rail at a higher pressure. Moreover, leakages involving the pressure reducer due to the allowance between cylinder and piston are reduced by the lesser pressure gradient between the lower and upper piston surfaces. Finally, allowing intermediate positions of the shutter in the pressure reducer permits a more accurate control of the intake flow from the tank and a remarkable reduction of the pressure oscillations due to control operations. A detailed description of the AMESim model of the system according the final layout is presented in section 4 (Fig. 2).

4 AMESIM MODEL OF THE CNG INJECTION SYSTEM

AMESim is a virtual prototyping software produced by IMAGINE S.A., which is oriented to lumped parameter modelling of physical elements, interconnected by ports enlightening the energy exchanges between pairs of elements and between an element and its environment. AMESim enables the modelling of components from different physical domains and the integration of these different elements in an overall system framework. It also guarantees a flexible architecture, capable of including new components defined by the users.

By assumption, the pressures distribution within the control chamber, the common rail and the injectors is uniform, and the elastic deformations of solid parts due to pressure changes are negligible. The pipes are considered as incompressible ducts with friction and a non uniform pressure distribution. Temperature variations are taken into account, affecting the pressure dynamics in each subcomponent. Besides, only heat exchanges through pipes are considered, by properly computing a thermal exchange coefficient. The tank pressure plays the role of a maintenance input, and it is modelled by a constant

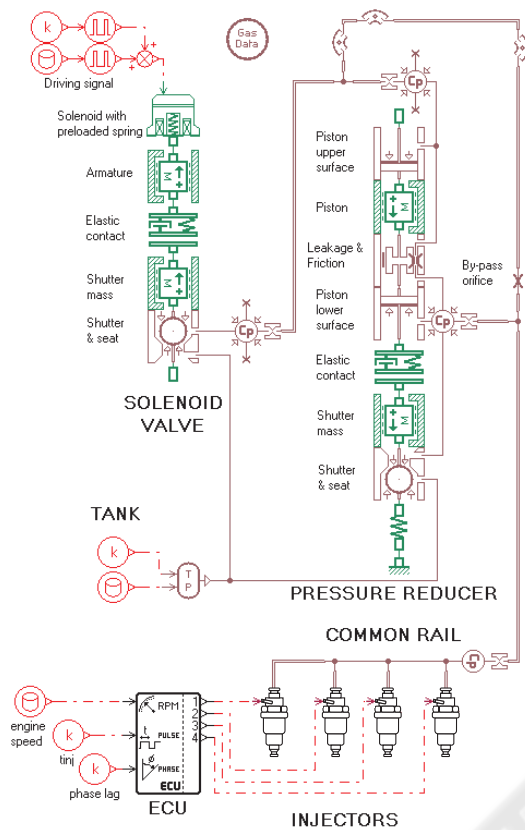


Figure 2: AMESim model of the CNG injection system.

pneumatic pressure source. To simplify the AMESim model construction some supercomponents have been suitably created, collecting elements within a single one.

4.1 Pressure Reducer and Common Rail

The main components for modelling the pressure reducer are the *Mass block with stiction and coulomb friction and end stops*, which computes the piston and the shutter dynamics through the Newton's second law of motion, a *Pneumatic ball poppet with conical seat*, two *Pneumatic piston*, and an *Elastic contact* modelling the contact between the piston and the shutter. The *Pneumatic piston* components compute the pressure forces acting upon the upper and lower piston surfaces. The viscous friction and leakage due to contact between piston and cylinder are taken into account through the *Pneumatic leakage and viscous friction* component, by specifying the length of contact, the piston diameter and the clearance. Finally, a *Variable volume with pneumatic chamber* is used to

compute the pressure dynamics as a function of temperature T and intake and outtake flows \dot{m}_{in} , \dot{m}_{out} , as well as of volume changes due to mechanical part motions, according to the following equation:

$$\dot{p} = \frac{RT}{V} \left(\dot{m}_{in} - \dot{m}_{out} + \rho \frac{dV}{dt} \right), \quad (1)$$

where p is the fuel pressure, ρ the fuel density and V the taken up volume. The same component is used to model the common rail by neglecting the volume changes.

Both pressure and viscous stresses contribute to drag forces acting on a body immersed in a moving fluid. In particular, the total drag acting on a body is the sum of two components: the pressure or form drag, due to pressure gradient, and the skin friction or viscous drag, i.e. *Drag force = Form drag + Skin friction drag*. By introducing a drag coefficient C_D depending on Reynolds number, the drag can be expressed in terms of the relative speed v (Streeter et al., 1998):

$$Drag = C_D \rho A v^2 / 2. \quad (2)$$

Moving shutters connecting two different control volumes are subject to both form drag and skin friction drag. The former one is properly computed by AMESim algorithms for a variety of shutters, considering different poppet and seat shapes. As for the latter, it is computed as a linear function of the fluid speed by the factor of proportionality. It can be obtained by noting that for a spherical body it holds *Form Drag = $2\pi D \mu v$* (Streeter et al., 1998), being μ the absolute viscosity and D the shutter diameter. The moving anchor in the solenoid valve experiences a viscous drag depending on the body shape. In particular, the drag coefficient of a disk is $C_D = 1.2$, and the skin friction drag can be computed using eq. 2. Since, by hypothesis, the anchor moves within a fluid with uniform pressure distribution, the form drag is neglected.

4.2 Pipes

The continuity and momentum equations are used to compute pressures and flows through pipes so as to take into account wave propagation effects. In case of long pipes with friction, a system of nonlinear partial differential equations is obtained, which is implemented in the *Distributive wave equation submodel of pneumatic pipe* component from the pneumatic library. This is the case of pipes connecting pressure reducer and common rail. The continuity and momentum equations can be expressed as follows (Streeter et al., 1998):

$$\frac{\partial \rho}{\partial t} + \rho \frac{\partial v}{\partial x} = 0, \quad (3)$$

$$\frac{\partial u}{\partial t} + \frac{\alpha^2 \rho}{\rho x} + \frac{f}{2d} u|u| = 0, \quad (4)$$

where α is the sound speed in the gas, d is the pipe diameter, f is the D'Arcy friction coefficient depending on the Reynolds number. AMESim numerically solves the above equations by discretization.

For short pipes, the *Compressibility + friction submodel of pneumatic pipe* from is used, allowing to compute the flow according the following equation:

$$q = \sqrt{\frac{2D\Delta p}{L\rho f}}, \quad (5)$$

where Δp is the pressure drop along the pipe of length L . The pipes connecting common rail and injectors are modelled in such a way.

Heat transfer exchanges are accounted for by the above mentioned AMESim components, provided that a heat transfer coefficient is properly specified. For a cylindrical pipe of length L consisting of a homogeneous material with constant thermal conductivity k and having an inner and outer convective fluid flow, the thermal flow Q is given by (Zucrow and Hoffman, 1976):

$$Q = \frac{2\pi k L \Delta T}{\ln \frac{r_o}{r_i}}, \quad (6)$$

where ΔT is the temperature gradient between the internal and external surfaces, and r_o and r_i are the external and internal radiuses, respectively. With reference to the outside surface of the pipe, the heat-transfer coefficient U is:

$$U_o = \frac{k}{r_o \ln \frac{r_o}{r_i}}. \quad (7)$$

4.3 Solenoid Valve and Magnetic Circuits

The AMESim model for the solenoid valve is composed of the following elements: a solenoid with preloaded spring, two moving masses with end stops subject to viscous friction and representing the magnet anchor and the shutter respectively, and a component representing the elastic contact between the anchor and the shutter. The intake section depends on the axial displacement of the shutter over the conical seat and is computed within the *Pneumatic ball poppet with conical seat* component, which also evaluates the drags acting on the shutter. The solenoid valve is driven by a peak-hold modulated voltage. The resulting current consists of a peak phase followed by a variable duration hold phase. The valve opening time is regulated by varying the ratio between the hold phase duration and signal period, namely the control

signal *duty cycle*. This signal is reconstructed by using a *Data from ASCII file signal source* that drives a *Pulse Width Modulation* component.

To compute the magnetic force applied to the anchor, a supercomponent (*Solenoid with preloaded spring* in Fig. 2) modelling the magnetic circuit has been suitably built, as described in the following. The magnetic flux within the whole magnetic circuit is given by the Faraday law:

$$\phi = (e_{ev} - R_{ev}i_{ev})/n, \quad (8)$$

where ϕ is the magnetic flux, R the n turns winding resistance, e_{ev} the applied voltage and i_{ev} the circuit current. Flux leakage and eddy-currents have been neglected. The magnetomotive-force *MMF* able to produce the magnetic flux has to compensate the magnetic tension drop along the magnetic and the air gap paths. Even though most of the circuit reluctance is applied to the air gap, nonlinear properties of the magnet, due to saturation and hysteresis, sensibly affect the system behaviour. The following equation holds:

$$MMF = MMF_s + MMF_a = H_s l_s + H_a l_a, \quad (9)$$

where H is the magnetic field strength and l is the magnetic path length, within the magnet and the gap respectively. The air gap length depends on the actual position of the anchor. The magnetic induction within the magnet is a nonlinear function of H . It is assumed that the magnetic flux cross section is constant along the circuit, yielding:

$$B = \phi/A_m = f(H_s) = \mu_0 H_a, \quad (10)$$

where A_m is the air gap cross section and μ_0 is the magnetic permeability of air. The $B - H$ curve is the hysteresis curve of the magnetic material. Arranging the previous equations yields to ϕ , B and H . The resulting magnetic force and circuit current are:

$$F_{ev} = A_m B^2 / \mu_0, \quad (11)$$

$$i_{ev} = MMF/n. \quad (12)$$

The force computed by the previous equation is applied to the mass component representing the anchor, so that the force balance can be properly handled by AMESim.

4.4 Injectors

The injectors are solenoid valves driven by the ECU in dependence of engine speed and load. The whole injection cycle takes place in a 720° interval with a delay between each injection of 180° . A supercomponent including the same elements as for the solenoid valve has been built to model the electro-injectors. The command signal generation is demanded to the ECU component, which provides a square signal driving each injector and depending on the current engine speed, injector timings and pulse phase angle.

5 CONTROLLER DESIGN

In designing an effective control strategy for the injection pressure it is necessary to satisfy physical and technical constraints. In this framework, model predictive control (MPC) techniques are a valuable choice, as they have shown good robustness in presence of large parametric variations and model uncertainties in industrial processes applications. They predict the output from a process model and then impress a control action able to drive the system to a reference trajectory (Rossiter, 2003). A 2nd order state space analytical model of the plant (Lino et al., 2006) is used to derive a predictive control law for the injection pressure regulation. The model trades off between accuracy in representing the dynamical behaviour of the most significant variables and the need of reducing the computational effort and complexity of controller structure and development. The design steps are summarized in the following. Firstly, the model is linearized at different equilibrium points, in dependence of the working conditions set by the driver power request, speed and load. From the linearized models it is possible to derive a discrete transfer function representation by using a backward difference method. Finally, a discrete Generalised Predictive Control (GPC) law suitable for the implementation in the ECU is derived from the discrete linear models equations.

By considering the *duty cycle* of the signal driving the solenoid valve and the rail pressure as the input u and output y respectively, a family of ARX models can be obtained, according the above mentioned design steps (Lino et al., 2006):

$$(1 - a_1 q^{-1})y(t) = (b_0 q^{-1} - b_1 q^{-2})u(t), \quad (13)$$

where q^{-1} is the shift operator and a_1, b_0, b_1 are constant parameters. The j -step optimal predictor of a system described by eq. 13 is (Rossiter, 2003):

$$\hat{y}(t + j|t) = G_j \Delta u(t + j - 1) + F_j y(t), \quad (14)$$

where G_j and F_j are polynomials in q^{-1} , and Δ is the discrete derivative operator. Let \mathbf{r} be the vector of elements $y(t + j)$, $j = 1, \dots, N$, depending on known values at time t . Then eq. (14) can be expressed in the matrix form $\hat{\mathbf{y}} = \mathbf{G}\tilde{\mathbf{u}} + \mathbf{r}$, being $\tilde{\mathbf{u}} = [\Delta u(t), \dots, \Delta u(t + N - 1)]^T$, and \mathbf{G} a lower triangular $N \times N$ matrix (Rossiter, 2003).

If the vector \mathbf{w} is the sequence of future reference values, a cost function taking into account the future errors can be introduced:

$$J = E \left\{ (\mathbf{G}\tilde{\mathbf{u}} + \mathbf{r} - \mathbf{w})^T (\mathbf{G}\tilde{\mathbf{u}} + \mathbf{r} - \mathbf{w}) + \lambda \tilde{\mathbf{u}}^T \tilde{\mathbf{u}} \right\}, \quad (15)$$

where λ is a sequence of weights on future control actions. The minimization of J with respect of $\tilde{\mathbf{u}}$ gives the optimal control law for the prediction horizon N :

$$\tilde{\mathbf{u}} = (\mathbf{G}^T \mathbf{G} + \lambda \mathbf{I})^{-1} \mathbf{G}^T (\mathbf{w} - \mathbf{r}). \quad (16)$$

At each step, the first computed control action is applied and then the optimization process is repeated after updating all vectors. It can be shown (Lino et al., 2006) that the resulting control law for the case study becomes:

$$\Delta u(t) = k_1 w(t) + (k_2 + k_3 q^{-1})y(t) + k_4 \Delta u(t - 1), \quad (17)$$

where $[k_1, k_2, k_3, k_4]$ depends on N .

6 SIMULATION AND EXPERIMENTAL RESULTS

To assess the effectiveness of the AMESim model in predicting the system behaviour, a comparison of simulation and experimental results has been performed. Since, for safety reasons, air is used as test fluid, the experimental setup includes a compressor, providing air at a constant input pressure and substituting the fuel tank. The injection system is equipped with four injectors sending the air to a discharging manifold. Moreover, a PC system with a National Instrument acquisition board is used to generate the engine speed and load signals, and a programmable MF3 development master box takes the role of ECU driving the injectors and the control valve.

Figure 3 refers to a typical transient operating condition, and compares experimental and simulation results. With a constant 40 bar input pressure, the system behaviour for a constant $t_j = 3$ ms injectors opening time interval, while varying engine speed and solenoid valve driving signal has been evaluated. The engine speed is composed of ramp profiles (Fig. 3(c)), while the *duty cycle* changes abruptly within the interval [2%, 12%] (Fig. 3(d)). Figures 3(a) and 3(b) show that the resulting dynamics is in accordance with the expected behaviour. A maximum error of 10% confirms the model validity.

After the validation process, the AMESim virtual prototype was used to evaluate the GPC controller performances in simulation by employing the AMESim-Simulink interface, which enabled us to export AMESim models within the Simulink environment. The interaction between the two environments operates in a *Normal* mode or a *Co-simulation* mode. As for the former, a compiled S-function containing the AMESim model is generated and included in the Simulink block scheme, and then integrated by the

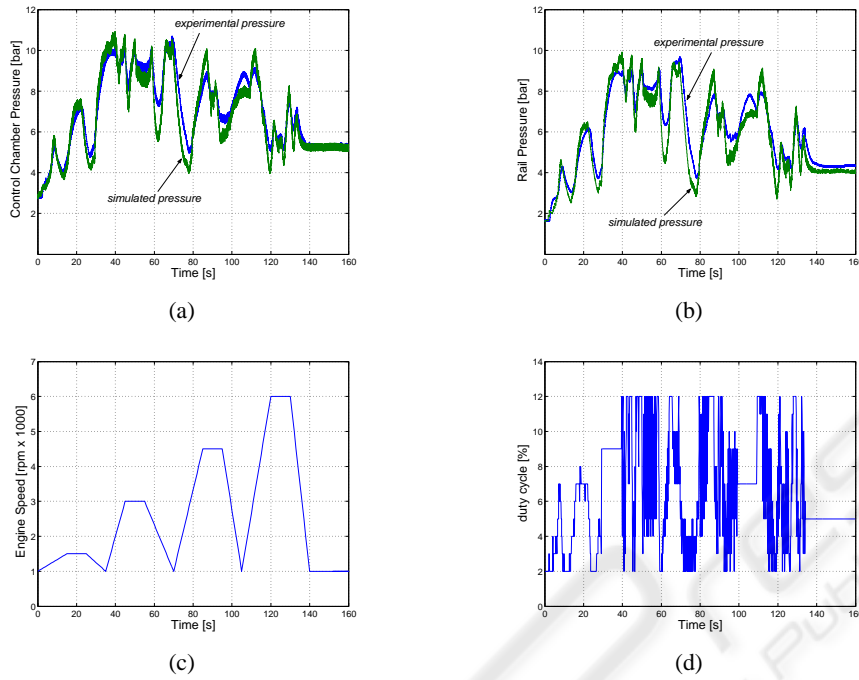


Figure 3: AMESim simulation and experimental results when varying *duty cycle*. and engine speed, with a constant $t_j = 3\text{ms}$; (a) control chamber pressure; (b) common rail pressure; (c) engine speed; (d) control signal *duty cycle*.

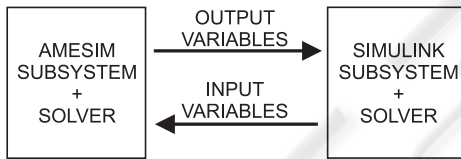


Figure 4: AMESim-MATLAB co-simulation interface.

Simulink solver. As for the latter, which is the case considered in this paper, AMESim and Simulink cooperate by integrating the relevant portions of models, as shown in figure 4.

The GPC controller was tuned referring to models linearized at the starting equilibrium point, according to design steps of Section 5. The test considered ramp variations of the engine speed and load, for the system controlled by a GPC with a $N = 5$ ($0.5s$) prediction horizon. The input air pressure from the compressor was always 30bar. The rail pressure reference was read from a static map depending on the working condition and had a sort of ramp profile as well. The final design step consisted in the application of the GPC control law to the real system.

In Fig. 5, the engine speed accelerates from 1100rpm to 1800rpm and then decelerates to

1100rpm, within a 20s time interval (Fig. 5(b)).

The control action applied to the real system guarantees a good reference tracking, provided that its slope does not exceed a certain value (Fig. 5(a), time intervals $[0, 14]$ and $[22, 40]$). Starting from time 14s, the request of a quick pressure reduction causes the control action to close the valve completely (Fig. 5(c)) by imposing a *duty cycle* equal to 0. Thanks to injections, the rail pressure (Fig. 5(a)) decreases to the final 5bar reference value, with a time constant depending on the system geometry; the maximum error amplitude cannot be reduced due to the actuation variable saturation. Fig. 5(d) shows the injectors' exciting time during the experiment. It is worth to note that simulation and experimental results are in good accordance, supporting the proposed approach.

7 CONCLUSIONS

In this paper, we presented a procedure for integrating different models and tools for a reliable design, optimization and analysis of a mechatronic system as a whole, encompassing the real process and the control system. The effectiveness of the methodology has been illustrated by introducing a practical case study involving the CNG injection system for internal com-

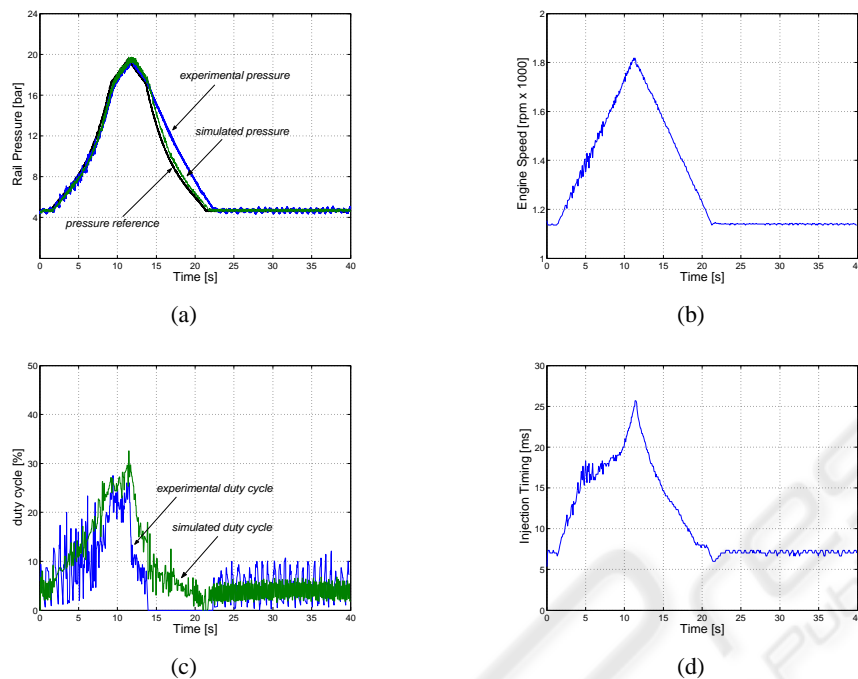


Figure 5: AMESim model and real system responses for speed and load ramp variations and a 30bar input pressure, when controlled by a GPC with $N = 5$; (a) common rail pressure; (b) engine speed (c) *duty cycle*; (d) injectors exciting time interval.

bustion engines. The design process was organized in few steps: analysis of different candidate configurations carried out with the help of virtual prototypes developed in the AMESim environment; design and performance evaluation of controllers designed on a simpler model of the plant employing the virtual prototypes; validation of the control law on the real system. The implementation of the control law on the real system represented a benchmark for the evaluation of performances of the approach. Experimental results gave a feedback of benefits of the integration of the mechanical and control subsystems design, and proved the validity of the methodology.

REFERENCES

- Ferretti, G., Magnani, G., and Rocco, P. (2004). Virtual Prototyping of Mechatronic Systems. *Annual Reviews in Control*, (28):193206.
- Lino, P., Maione, B., Amorese, C., and DeMatthaeis, S. (2006). Modeling and Predictive Control of a New Injection System for Compressed Natural Gas Engines. In *IEEE CCA 2006 International Conference*, Munich, Germany.
- Maione, B., Lino, P., DeMatthaeis, S., Amorese, C., Mandoro, D., and Ricco, R. (2004). Modeling and Control of a Compressed Natural Gas Injection System. *WSEAS Transactions on Systems*, 3(5):2164–2169.
- Paynter, H. (1960). *Analysis and Design of Engineering Systems*. M.I.T. Press, Cambridge, MA.
- Rossiter, J. (2003). *Model-Based Predictive Control: a Practical Approach*. CRC Press, New York.
- Stobart, R., A.May, Challen, B., and Morel, T. (1999). New Tools for Engine Control System Development. *Annual Reviews in Control*, (23):109–116.
- Streeter, V., Wylie, K., and Bedford, E. (1998). *Fluid Mechanics*. McGraw-Hill, New York, 9th edition.
- IMAGINE S.A. (2004). *AMESim User Manual v4.2*. Roanne, France.
- van Amerongen, J. and Breedveld, P. (2003). Modelling of Physical Systems for the Design and Control of Mechatronic Systems. *Annual Reviews in Control*, (27):87–117.
- Zucrow, M. and Hoffman, J. (1976). *Gas Dynamics*. John Wiley & Sons, New York.